R.R.M. DE BARROS[1], A.B. NOVAES JR.[1], B. ASSENZA[2], A. PIATTELLI[3]

[1] PhD, DDS, Department of Bucco-Maxillo-Facial Surgery and Traumatology and Periodontology, School of Dentistry of Ribeirão Preto, University of São Paulo, Ribeirão Preto, SP, Brazil
[2] Private practice, Milan, Italy
[3] PhD, Department of Oral Medicine and Oral Pathology, School of Dentistry, University of Chieti-Pescara, Chieti, Italy

Nanomechanical properties of bone around cement-retained abutment implants. A minipig study

TO CITE THIS ARTICLE
Barros RRM, Novaes Jr. AB, Assenza B, Piattelli A. Nanomechanical properties of bone around cement-retained abutment implants. A minipig study. J Osseointegr 2015;7(2):33-39.

ABSTRACT

Aim The nanomechanical evaluation can provide additional information about the dental implants osseointegration process. The aim of this study was to quantify elastic modulus and hardness of bone around cemented-retained abutment implants positioned at two different crestal bone levels.
Materials and methods The mandibular premolars of 7 minipigs were extracted. After 8 weeks, 8 implants were inserted in each animal: crestally on one side of the mandible and subcrestally on the other (crestal and subcrestal groups). Functional loading were immediately provided with abutments cementation and prostheses installation. Eight weeks later, the animals euthanasia was performed and nanoindentation analyses were made at the most coronal newly formed bone region (coronal group), and below in the threaded region (threaded group) of histologic sections.
Results The comparisons between subcrestal and crestal groups did not achieve statistical relevance; however the elastic modulus and hardness levels were statistically different in the two regions of evaluation (coronal and threaded).
Conclusions The crestal and subcrestal placement of cement-retained abutment implants did not affect differently the nanomechanical properties of the surrounding bone. However the different regions of newly formed bone (coronal and threaded groups) were extremely different in both elastic modulus and hardness, probably reflecting their differences in bone composition and structure.

KEYWORDS Abutment connection; Animal model; Dental implant; Nanomechanical properties.

INTRODUCTION

The modifications of implant surface on topography, chemistry, and surface energy/hydrophilicity play a decisive hole in the achievement of high levels of osseointegration (1-3), however other aspects may interfere on crestal bone preservation along time (4). The study of implant-abutment connections and their positioning in relation to the crestal bone aims to minimize crestal bone loss in order to guarantee the long-term success and the aesthetic restorative outcome of dental implants.
Cement-retained abutment (CRA) implants conversely to the screw-retained abutment (SRA) implants presented their microgaps at the abutment-implant interface completely filled by the fixation cement as observed by the Scanning Electron Microscopy (SEM) analysis (5). *In vitro* studies showed that neither fluid nor bacterial penetration was observed in CRA implants, whereas in all SRA implants penetration of fluids and bacteria was observed inside the internal cavity of the implant (5, 6). The contamination of the implant-abutment interface as an empty space could potentially cause significant crestal bone loss, impairing the final result (7-10).
Some CRA implants exhibit a double retention connection (mechanical and chemical) of the abutment and transmucosal element, in order to bring the sealing interface outside of the peri-implant tissues, collaborating to their healing and health. The dual retention consists in the coupling of the component and transmucosal implant without screws in addition to the chemical bonding of the abutment within the implant (11). This approach can reduce the micromovements and the inflammatory agents nearby the crestal bone in order to achieve lower rates of bone resorption (12).
These implants were previously evaluated by conventional histologic techniques after immediate loading in the minipig model and their subcrestal positioning achieved statistically better results when compared to the crestal group in terms of crestal bone remodeling (1.17 x 1.63 mm), bone density (52.39 x 45.22%) and bone to implant

contact (54.13 x 42.46%) (11); however additional information could be obtained by new evaluation techniques.

Osseointegration was originally defined as the direct bone to implant contact (BIC) without interposed soft tissues (13) and has been quantified throughout the years by histology/histomorphometry methods. However, it has now been discussed that this evaluation technique may not capture the entire phenomenon (14). The advances in the ability to predict implant success demand anatomically specific measures of the local mechanical environment (15). Clinically, an important factor to take into consideration is the load-bearing capability of the implant, which involves the mineralization status of the newly formed bone. The mineral content has been shown to correlate with bone lamellar-level microhardness (16-18). Thus it would be further beneficial to evaluate the bone nanomechanical properties of the contacting bone to the implants, because this could provide additional information regarding the quality of bone, which may possibly correlate to the so called implant secondary (biologic) stability (14).

Several investigators have explored regional and anatomical variation in the macroscopic mechanical properties of human cortical and trabecular bone (19-22). However, parallel studies at the microscopic level are far less numerous.

Nanoindentation has recently been validated as an accurate and reproducible technique to measure lamellar-level bone elastic properties (15). Unfortunately, a comprehensive evaluation of the lamellar-level elastic properties of bone tissue around dental implants remains extremely scarce.

Hence, the objective of this study was to quantify the elastic properties of bone tissue around specific cement-retained dental implants positioned at two different levels in relation to the crestal bone.

MATERIALS AND METHODS

Animals and surgical procedures

A total of 7 minipigs (Minipig BR-1; Minipig Comércio e Desenvolvimento; Campina do Monte Alegre, SP, Brasil) (age: about 18 months old; weight: 20 to 30 kg) were selected for the study. They received antiparasitic treatment, vitamins, a full series of vaccines and prophylactic dental hygiene treatment with ultrasonic points (Cavitron 3000, Dentsply Mfg. Co., York, PA, USA). All the surgical procedures were performed under general anesthesia and the whole experimental phase *in vivo* was accompanied by a veterinarian. The Ethics Committee for Animal Research of the Catholic Pontifical University of Paraná - Brazil approved the study (protocol number: 561).

Food was withheld in the night preceding surgeries. The animals were pre-anesthetized with Azaperone (Destress, DES-Vet; São Paulo, SP, Brazil; 1 mg/kg, intramuscularly) and after 20 minutes, were anesthetized with Ketamine (Dopalen, Vetbrands; Jacareí, SP, Brazil; initial dose of 5 mg/kg, intramuscularly). Throughout the period of deep sedation, the animals were monitored for heart rate, respiratory rate, temperature, palpebral and intestinal reflexes.

The animals underwent two surgical interventions. The first intervention was the extraction of the mandibular premolars on both sides of the mandible, which was performed with bilateral full-thickness flap elevation. In order to avoid any damage to the neighboring bony walls, the teeth were sectioned in a buccolingual direction at the furcation area and the roots were extracted individually with the use of a periotome and forceps. In some animals, the tooth germs that were present in the referred regions were also extracted. The flaps were then repositioned and sutured with absorbable sutures (Vicryl, Ethicon, Inc., Johnson & Johnson Company, São José dos Campos, SP, Brazil).

After 8 weeks of healing, implant placement surgeries were performed. Horizontal incisions were made on the crest of the ridges, from the distal of the canines to the mesial of the first molars and after the full-thickness flaps elevation, the complete healing of the alveolar ridges was observed (Fig. 1). The implants were placed according to the manufacturer's guidelines. Four cement-retained abutment (CRA) implants of 4.1 mm in diameter and 10 mm in length (Bone System, Milano, Italy) were placed at the crestal bone level on one side of the jaw (crestal group). Contralaterally, CRA implants of 4.1 mm in diameter and 8 mm in length were placed 1.5 mm below the crestal bone level (subcrestal group). Surgical guides were manufactured to standardize both the angle and the distance between the implants. The implants were placed with distances of 2 to 3 mm between them (Fig. 2). The surface of all the implants were sandblasted and etched with Ecotek treatment.

Immediately after implant placement, the transfers were

FIG. 1 The alveolar ridge completely healed after the full-thickness flap elevation for implant placement.

FIG. 2 Cement-retained abutment (CRA) implants placed on one side of the jaw. Distances of 2 to 3mm between the adjacent implants were left.

FIG. 3 Metal prostheses were adapted on the implants on the same day of their placement.

adapted for the impressions and the flaps were sutured with absorbable sutures.

The transmucosal element was fitted with friction using a special atraumatic tool, which can exert the force required for the coupling, without causing damage to hard and soft tissues. Then the abutments were cemented through the transmucosal element. With this element, the cementation occurred outside of the soft tissue, minimizing the risk of peri-implant gingiva contamination. The cement excess leaked to the abutment base and was easily removed with a pellet of cotton or gauze, given its semi fluid consistency in the presence of oxygen.

Metal prostheses were manufactured in the laboratory and the distance between the contact point of the adjacent crowns to the crestal bone apex was standardized in 3 mm. Finally they were adapted on the implants (Fig. 3).

After each surgical intervention, tramadol was used (50 mg/ml) with a dosage of 3 mg/kg as analgesic therapy and ketoprofen (20 mg) with a dosage of 1 pil/20 kg as anti-inflammatory therapy. The animals also received antibiotic therapy (Stomorgyl 10, Merial Animal Health Ltd., Paulínia, SP, Brazil), 1 pil/10 kg for 10 days.

The animals were fed with moist pig ration for 14 days, when the sutures were removed. The healing was evaluated weekly and plaque control was maintained by flushing the oral cavity with 0.12% chlorhexidine gluconate. The remaining teeth received ultrasonic instrumentation monthly.

During the experimental period, the animals received water without restriction, and were fed accordingly (S4, Bravisco, Bastos, SP, Brazil), in a daily amount equivalent to 2% of the weight of the animals. Eight weeks later, the euthanasia of the animals was performed with a lethal dose of thiopental (Sigma Aldrich, Canada).

Sample preparation and Ground Sectioning

The hemi-mandibles were removed, dissected and fixed in a 4% solution of formalin at pH 7 for 10 days and transferred to a solution of 70% ethanol until processing. The specimens were dehydrated in ascending ethanol concentrations up to 100%, infiltrated and embedded in LR White resin (London Resin Company, Berkshire, England) according to the manufacturer's instructions. After polymerization, the embedded samples were cut at the center of the implant along its long axis with a diamond saw (Isomet 2000; Buehler, Ltd., Lake Bluff, IL, USA) and subjected to grinding and polishing using a series of abrasive papers to a final thickness of approximately 30 µm; for scratch removal, further polishing was performed with diamond suspensions of 9 to 1 µm particle size (Buehler, Lake Bluff, IL, USA).

Nanoindentation

Nanoindentation was performed with a nanoindenter (Hysitron, Minneapolis, MN) equipped with a Berkovich diamond 3-sided pyramid tip (23). A wax chamber was created above the acrylic plate around the implant-bone perimeter, so that tests were performed in distilled water (24). A loading profile was developed with a peak load of 300 mN at a rate of 60 mN/s, followed by a holding time of 10 seconds and an unloading time of 2 seconds. The extended holding period allowed bone to relax to a more linear response, so that no tissue creep effect was occurring in the unloading portion of the profile (ISO 14577-4). Therefore, from each indentation, a load-displacement curve was obtained.

Sixty indentations were performed in ten selected histologic sections, representative of the experimental groups. They were performed in a newly formed bone to 0.1 mm from the implant surface with a distance of at least 10 µm from each other so that no interactions between them affected the mechanical results. Thirty of them were made at the most coronal newly formed bone region (coronal group), and thirty below in the threaded region (threaded group), composing two different evaluation regions.

Bone tissue was detected by imaging under the light microscope (Hysitron TI 950, Minneapolis, MN, USA) (25), and the indentations were performed in the selected areas. From each analyzed load-displacement curve, reduced modulus (GPa) and hardness (GPa) of bone tissue were computed and its elastic modulus Eb (GPa) was calculated as follows:

$$\frac{1}{E_r} = \frac{1-\nu^2}{E} + \frac{1-\nu_i^2}{E_i}$$

where E_r is the reduced modulus (GPa), ν (0.3) is the Poisson's ratio for cortical bone, and E_i (1140GPa) and ν_i (0.07) are the elastic modulus and Poisson's ratio for the indenter, respectively (15, 26, 27).

Statistical analysis

The collected data of the nanomechanical properties were ranked and the Repeated Measures ANOVA was used to compare the results between the crestal and subcrestal groups and the Wilcoxon Matched Pairs was used to compare the intra-group results of the coronal and threaded regions. All statistical analyses were performed at a 95% confidence level.

RESULTS

The mean ± SD elastic modulus for the subcrestal group was 10.31 ± 7.65 GPa at the coronal region and 7.37 ± 6.37 GPa at the threaded region, where the bone is in contact with the implant; for the crestal group, it was 11.21 ± 9.71 GPa at the coronal region and 7.83 ± 7.07 GPa at the threaded region. The comparisons between subcrestal and crestal groups did not achieve statistically significant differences, however, the levels observed in the different regions of evaluation (coronal and threaded) inside the same group of analysis (crestal or subcrestal) were statistically different (Table 1; Fig. 4).
Besides, the mean ± SD hardness for the subcrestal group was 0.58 ± 0.43 GPa at the coronal region and 0.34 ± 0.30 GPa at the threaded region; for the crestal group, it was 0.57 ± 0.50 GPa at the coronal region and 0.35 ± 0.30 GPa at the threaded region. In a similar way to the previous parameter, the comparisons of hardness levels between subcrestal and crestal groups did not achieve statistically significant differences, while the comparisons between the different regions of evaluation (coronal and threaded) inside the same group of analysis (crestal or subcrestal) achieved statistically significant differences (Table 2; Fig. 5).

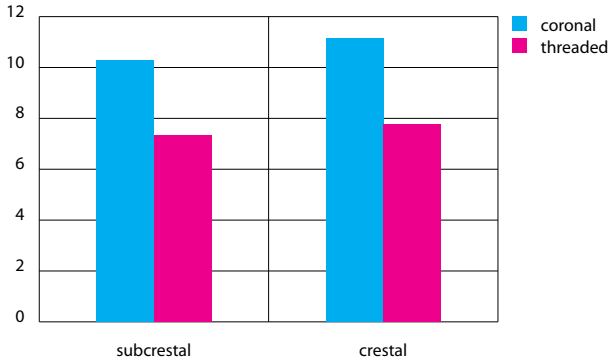

FIG. 4 Elastic modulus. Observe the intra-group analysis (subcrestal and crestal). The coronal regions showed statistical superior results when compared to the threaded regions in both groups individually

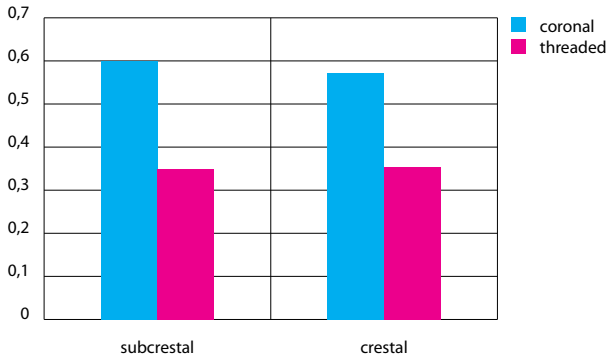

FIG. 5 Hardness. Observe the intra-group analysis (subcrestal and crestal). The coronal regions showed statistical superior results when compared to the threaded regions in both groups individually.

	sub / C	sub / T	cre / C	cre / T
mean	10,3144*	7,374755*	11,21722**	7,839413**
median	7,654572	6,739503	9,713403	7,07983
SD	9,588083	4,028665	6,504221	5,710143
Statistically significant differences (Wilcoxon Matched Pairs): (*) p= 0.0005 (**) p<0.0001				

TABLE 1 Elastic Modulus (GPa) in subcrestal (sub) and crestal (cre) groups and in the different regions of evaluation, coronal (C) and threaded (T).

	sub / C	sub / T	cre / C	cre / T
mean	0,598079*	0,349765*	0,576298**	0,35899**
median	0,435486	0,309296	0,504978	0,307093
SD	0,569275	0,190708	0,353282	0,259207
Statistically significant differences (Wilcoxon Matched Pairs): (*) p= 0.0005 (**) p<0.0001				

TABLE 2 Hardness (GPa) in subcrestal (sub) and crestal (cre) groups and in the different regions of evaluation, coronal (C) and threaded (T).

DISCUSSION

Currently, the technology in dental implants reached high levels and the combination of multiple variables in a single implant makes its evaluation and comparison with other implants increasingly difficult and complex. The determination of the bone to implant contact by histologic/histomorphometric techniques has been considered a low sensitive evaluation because of its being a two-dimensional one that provides specific information of a single moment of the osseointegration process.

Clinically, an important factor to take into consideration is the stability of the implant that will withstand dynamic loading. Evidently, this would require simultaneous new bone formation, and the study of the mineralization level of forming bone may provide valuable information.

The nanoindentation method allows the investigation of the mechanical properties of variable samples at the nanoscale level. It is possible to assess the reduced elastic modulus and hardness of bone specimens.

Elastic modulus and hardness are both conceptually and physically distinct. Elastic modulus characterizes rate-independent reversible material behavior, while hardness describes resistance to plastic deformation. Microhardness was found to be an accurate and reliable measure of the degree of mineralization (28).

The macroscopic mechanical properties of bones are determined by composition as well as nanostructural (lamellae), microstructural (osteon/trabecular pocket) and structural (compacta/trabecula) organization (29-31). In general, it has been suggested that the elastic modulus correlates with hardness (17). However, it is also a fact that this correlation is bone type and depth dependent (32).

Zysset et al. (28) found that the elastic modulus of human bone strongly depend on tissue type, anatomical location and individual. The difference in elastic modulus obtained between compact and trabecular tissue may be attributed to variations in canalicular porosity or mineralization of the extracellular matrix (30, 33). According to their findings the difference in elastic properties found between anatomical locations may involve turnover rate and osteon type. A higher turnover rate reduces the mean age of the osteons and therefore reduces mineralization and the associated elastic properties. According to Ascenzi et al. studies (34-36), a different distribution of osteon types, distinguished by predominant collagen fiber orientation, may be present in one bone region as compared to another which may also lead to distinct average mechanical properties.

The present study investigated the nanomechanical properties of bone around cement-retained abutment implants placed crestally or subcrestally in the mandible of minipigs and immediately loaded. The positions of installation, differently from the previous study that evaluated the osseointegration in terms of bone to implant contact percentages (11), did not reflect in statistically significant differences in elastic modulus or hardness levels. In other words the presence of the implant-abutment interface at the bone crest or below the bone crest did not interfere with the nanomechanical properties of the newly formed bone. However, the comparison of two different regions of bone, the most coronal newly formed bone above the threads of the implant and the newly formed bone in close contact with the implant threads, in subcrestal and crestal groups individually, showed extremely significant statistical relevance. A plausible explanation for this finding is defined by different types of bone in these regions. The coronal bone is usually a more compact bone while the bone of the lower part bordering the implant threads is generally more trabecular.

Many investigators have concluded that cortical bone tissue elastic moduli are greater than trabecular tissue using microtesting techniques (37-39), but those studies were limited by the unquantified interaction of porosity, microarchitecture, and lamellar-level material properties in defining microspecimen mechanical properties. This represents an advantage of the nanoindentation method that uses a micron resolution, permitting the mechanical properties test at a scale independent of microstructural influences. Hoffler et al. (15) evidenced with lamellar-level nanoindentation observation that the elastic properties of cortical bone are greater than trabecular bone which is in accordance to the present results. The heterogeneity of bone lamellar-level elastic and hardness properties is likely related to the mineral, collagenous, and noncollagenous protein composition. However, the point of great interest is that these differences in constituency reflect differential metabolic demands, which may influence the process of remodeling. The lower properties of trabecular bone likely reflect elevated rates of bone turnover and coincidental decreased mineral content (15). It is also known that there is a variation in collagen fiber orientations in both cortical and trabecular bone measurements, and that the trabecular bone owns a more complex architecture. In fact the loading of the implants with immediate prostheses also affects the orientation of collagen fibers (40). However, the effect of these different distributions of collagen fiber orientation within microstructural groups is unknown and may be ascertained in future studies.

Interestingly, Hoffler et al. (15) also showed that primary lamellar bone and Haversian bone are mechanically similar and differ only morphologically. This information supports the immediate loading protocol of dental implants, as the primary bone have sufficient strength to withstand the mechanical forces required, even if newly formed bone. Another factor that should be taken into consideration, which may influence the bone mechanical property, is the alignment of the hydroxyapatite crystal (41). Nagisa et al. (42) have stated that hydroxyapatite crystals realign themselves based on the direction of the load they bear. The static and dynamic load-bearing

properties of each implant systems are unique because of the different macrogeometric designs of the threads (43). Thus, it is natural to speculate that different hydroxyapatite alignment around the implant threads may have had significant influence on the outcomes. The studies about the nanomechanical properties of bone around the implants are still very scarce, which makes the discussion between them difficult, since they have such different aims and methodologies. However, it is important to consider that nanoindentation could provide additional information regarding the bone quality, and this may possibly correlate to implant secondary stability. Jimbo et al. (14), for example, compared a nanoscale hydroxyapatite (HA)-coated implant to a grit-blasted, acid-etched, and heat-treated implant. No statistical differences were found between test and control surfaces in the histomorphometric results (bone-to-implant contact percentage). However, both the rank elastic modulus and rank hardness were significantly enhanced for the HA group relative to the control group. The authors suggested that the presence of nano HA had an effect at both the immediate interfacial regions and the relatively distant regions. With the nanoindenter, the capabilities of the nano HA to strengthen bone quality were demonstrated, validating the author's hypothesis that nanoscale HA-coated implant surfaces will hasten the quality of osseointegration.

CONCLUSION

The analysis of the nanomechanical properties of bone around dental implants may provide valuable and complementary information about the osseointegration process and load-bearing capability. The subcrestal and crestal placement of cemented-retained dental implants did not significantly affect the elastic modulus and hardness levels. However it can be concluded that the different positions of bone around implants, the most coronal newly formed bone above the threads and the newly formed bone in close contact with the implant threads, was extremely different in terms of nanomechanical properties, probably reflecting their differences in bone composition and structure.

ACKNOWLEDGEMENTS

This study was supported in part by FAPESP (process numbers 2010/19035-0 and 2010/19737-5). The authors wish to thank P. G. Coelho and G. Freitas for their respective contributions.

REFERENCES

1. Albrektsson T, Wennerberg A. Oral implant surfaces: Part 1d Review focusing on topographic and chemical properties of different surfaces and in vivo responses to them. Int J Prosthodont 2004;17:536-43.
2. Buser D, Broggini N, Wieland M, Schenk RK, Denzer AJ, Cochran DL, Hoffmann B, Lussi A, Steinemann SG. Enhanced bone apposition to a chemically modified SLA titanium surface. J Dent Res 2004;83:529-33.
3. Sul YT, Kang BS, Johansson C, Um HS, Park CJ, Albrektsson T. The roles of surface chemistry and topography in the strength and rate of osseointegration of titanium implants in bone. J Biomed Mater Res A 2009;89:942-50.
4. Oh TJ, Yoon J, Misch CE, Wang HL. The causes of early implant bone loss: Myth or science? J Periodontol 2002;73:322-33.
5. Piattelli A, Scarano A, Paolantonio M, Assenza B, Leghissa GC, Di Bonaventura G, Catamo G, Piccolomini R. Fluids and microbial penetration in the internal part of cement-retained versus screw-retained implant-abutment connections. J Periodontol 2001;72:1146-50.
6. Assenza B, Tripodi D, Scarano A, Perrotti V, Piattelli A, Iezzi G, D'Ercole S. Bacterial leakage in implants with different implant-abutment connections: an in vitro study. J Periodontol 2012;83:491-7.
7. Broggini N, McManus LM, Hermann JS, Medina R, Schenk RK, Buser D, Cochran DL. Periimplant inflammation defined by the implant-abutment interface. J Dent Res 2006;85:473-8.
8. Todescan FF, Pustiglioni FE, Imbronito AV, Albrektsson T, Gioso M. Influence of the microgap in the periimplant hard and soft tissues: A histomorphometric study in dogs. Int J Oral Maxillofac Implants 2002;17:467-72.
9. Piattelli A, Vrespa G, Petrone G, Iezzi G, Annibali S, Scarano A. Role of the microgap between implant and abutment: A retrospective histologic evaluation in monkeys. J Periodontol 2003;74:346-52.
10. Elian N, Bloom M, Dard M, Cho SC, Trushkowsky RD, Tarnow D. Effect of interimplant distance (2 and 3 mm) on the height of interimplant bone crest: a histomorphometric evaluation. J Periodontol 2011;82:1749-56.
11. Barros RRM, Novaes Jr. AB, Papalexiou V, Luczyszyn SM, Papalexiou SN, Ramos CMG, Almeida ALG, Assenza B, Piattelli A. Evaluation of contiguous implants with cement-retained implant-abutment connections. A minipig study. J Osseointegr 2014;1:3-10.
12. Lazzara RJ, Porter SS. Platform Switching: A New Concept in Implant Dentistry for Controlling Postrestorative Crestal Bone Levels. Int J Periodontics Restorative Dent 2006;26:9-17.
13. Albrektsson T. Hard tissue implant interface. Aust Dent J 2008;53:S34-S38.
14. Jimbo R, Coelho PG, Bryington M, Baldassarri M, Tovar N, Currie F, Hayashi M, Janal MN, Andersson M, Ono D, Vandeweghe S, Wennerberg A. Nano Hydroxyapatite-coated implants improve bone nanomechanical properties. J Dent Res 2012;91:1172-77.
15. Hoffler CE, Moore KE, Kozloff K, Zysset PK, Brown MB, Goldstein SA. Heterogeneity of bone lamellar-level elastic moduli. Bone 2000;26:603-9.
16. Amprino R. Investigations on some physical properties of bone tissue. Acta Anat 1958;34:161-86.
17. Evans GP, Behiri JC, Currey JD, Bonfield W. Microhardness and Young's modulus in cortical bone exhibiting a wide range of mineral volume fractions, and in a bone analogue. J Mater Sci Mater Med 1990;1:38-43.
18. Hodgskinson R, Currey JD, Evans GP. Hardness, an indicator of the mechanical competence of cancellous bone. J Orthop Res 1989;7:754-8.
19. Amling M, Herden S, Posl M, Hahn M, Ritzel H, Delling G. Heterogeneity of the skeleton: Comparison of the trabecular microarchitecture of the spine, the iliac crest, the femur, and the calcaneus. J Bone Miner Res 1996;11:36-45.
20. Brown TD, Ferguson Jr AB. Mechanical property distributions in the cancellous bone of the human proximal femur. Acta Orthop Scand 1980;51:429-37.
21. Goldstein SA, Wilson DL, Sonstegard DA, Matthews LS. The mechanical properties of human tibial trabecular bone as a function of metaphyseal location. J Biomech 1983;16:965-9.
22. Ciarelli MJ, Goldstein SA, Kuhn JL, Cody DD, Brown MB. Evaluation of orthogonal mechanical properties and density of human trabecular bone from the major metaphyseal regions with materials testing and computed tomography. J Orthop Res 1991;9:674-82.

23. Baldassarri M, Bonfante E, Suzuki M, Marin C, Granato R, Tovar N, Coelho PG. Mechanical properties of human bone surrounding plateau root form implants retrieved after 0.3-24 years of function. J Biomed Mater Res B Appl Biomater. 2012;100B:2015-21.
24. Wallace JM. Applications of atomic force microscopy for the assessment of nanoscale morphological and mechanical properties of bone. Bone 2012; 50:420-7.
25. Butz F, Aita H, Wang CJ, Ogawa T. Harder and stiffer bone osseointegrated to roughened titanium. J Dent Res 2006;85:560-5.
26. Oliver WC, Pharr GM. An improved technique for determining hardness and elastic-modulus using load and displacement sensing indentation experiments. J Mater Res 1992;7:1564-83.
27. Hoffler CE, Guo XE, Zysset PK, Goldstein SA. An application of nanoindentation technique to measure bone tissue lamellae properties. J Biomech Eng 2005; 127:1046-53.
28. Zysset PK, Guo XE, Hoffler CE, Moore KE, Goldstein SA. Elastic modulus and hardness of cortical and trabecular bone lamellae measured by nanoindentation in the human femur. J Biomech 1999;32:1005-12.
29. Ascenzi A. The micromechanics versus the macromechanics of cortical bone-A comprehensive presentation. J Biomech Eng 1988;110: 357-63.
30. Currey JD. The effect of porosity and mineral content on the Young's modulus of elasticity of compact bone. J Biomech 1988; 21:131-9.
31. Martin RB, Ishida J. The relative effects of collagen fiber orientation, porosity, density, and mineralization of bone strength. J Biomech 1989;22: 419-26.
32. Hengsberger S, Kulik A, Zysset P. Nanoindentation discriminates the elastic properties of individual human bone lamellae under dry and physiological conditions. Bone 2002;30:178-84.
33. 31Schaffler MB, Burr DB. Stiffness of compact bone: effects of porosity and density. J Biomech 1988;21:13-6.
34. Ascenzi A, Bonucci E. The tensile properties of single osteons. Anat Rec 1967;158:375-86.
35. Ascenzi A, Baschieri P, Benvenuti A. The bending properties of single osteons. J Biomech 1990;23:763-71.
36. Ascenzi A, Baschieri P, Benvenuti, A. The torsional properties of single selected osteons. J Biomech 1994;27: 875-84.
37. Choi K, Goldstein SA. A comparison of the fatigue behavior of human trabecular and cortical bone tissue. J Biomech 1992;25:1371-81.
38. Choi K, Kuhn JL, Ciarelli MJ, Goldstein SA. The elastic moduli of human subchondral, trabecular, and cortical bone tissue and the size dependency of cortical bone modulus. J Biomech 1990;23:1103-13.
39. Rho JY, Ashman RB, Turner CH. Young's modulus of trabecular and cortical bone material: Ultrasonic and microtensile measurements. J Biomech 1993;26:111-9.
40. Traini T, Neugebauer J, Thams U, Zöller JE, Caputi S, Piattelli A. Peri-implant bone organization under immediate loading conditions: collagen fiber orientation and mineral density analyses in the minipig model. Clin Implant Dent Relat Res 2009;11:41-51.
41. Viswanath B, Raghavan R, Gurao NP, Ramamurty U, Ravishankar N. Mechanical properties of tricalcium phosphate single crystals grown by molten salt synthesis. Acta Biomater 2008;4:1448-54.
42. Nagisa N, Nakano T, Hashiguchi N, Fujitani W, Umakoshi Y, Shimahara M. Analysis of biological apatite orientation in rat mandibles. Oral Sci Int 2010;7: 19-25.
43. Hansson S, Werke M. The implant thread as a retention element in cortical bone: The effect of thread size and thread profile: A finite element study. J Biomech 2003;36:1247-58.